

We are IntechOpen, the world's leading publisher of Open Access books Built by scientists, for scientists

6,900

Open access books available

186,000

International authors and editors

200M

Downloads

Our authors are among the

154

Countries delivered to

TOP 1%

most cited scientists

12.2%

Contributors from top 500 universities



WEB OF SCIENCE™

Selection of our books indexed in the Book Citation Index
in Web of Science™ Core Collection (BKCI)

Interested in publishing with us?
Contact book.department@intechopen.com

Numbers displayed above are based on latest data collected.
For more information visit www.intechopen.com



Copper Complexes as Influenza Antivirals: Reduced Zebrafish Toxicity

Kelly L. McGuire, Jon Hogge, Aidan Hintze, Nathan Liddle, Nicole Nelson, Jordan Pollock, Austin Brown, Stephen Facer, Steven Walker, Johnny Lynch, Roger G. Harrison and David D. Busath

Abstract

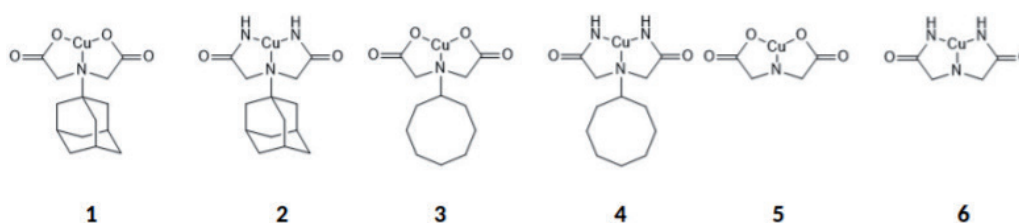
Copper complexes have previously been developed to target His37 in influenza M2 and are effective blockers of both the wild type (WT) and the amantadine-resistant M2S31N. Here, we report that the complexes were much less toxic to zebrafish than CuCl_2 . In addition, we characterized albumin binding, mutagenicity, and virus resistance formation of these metal complexes, and employed steered molecular dynamics simulations to explore whether the complexes would fit in M2. We also examined their anti-viral efficacy in a multi-generation cell culture assay to extend the previous work with an initial-infection assay, discovering that this is complicated by cell culture medium components. The number of copper ions binding to bovine serum albumin (BSA) correlates well with the number of surface histidines and BSA binding affinity is low compared to M2. No mutagenicity of the complexes was observed when compared to sodium azide. After 10 passages of virus in MDCK culture, the EC_{50} was unchanged for each of the complexes, i.e. resistance did not develop. The simulations revealed that the compounds fit well in the M2 channel, much like amantadine.

Keywords: medicinal metals, proton transport, plaque assay, Ames, CTX, CPE

1. Introduction

The influenza A M2 protein is a homotetrameric channel [1] that is particularly selective for protons [2] and is essential for uncoating of the virus [3]. The proton selectivity is due to the cluster of His37 imidazole side chains in the channel [4, 5]. This channel has been a primary antiviral target. Amantadine (AMT) and rimantadine (RMT) were highly successful as M2 blockers [6–8], but they became ineffective in 2005 when a mutation from serine to asparagine at residue 31 (S31N) in M2 occurred [9, 10].

Attempts have been made to develop variants of AMT, RMT and others that could block the V27A, L26F, or S31N mutations [11–14]. We explored a different approach that could, in theory, target all functional forms of M2 [15].

**Figure 1.**

Copper complexes with the functional groups iminodiacetate or iminodiacetamide extended via the amine to either AMT or CO.

Drawing from the observation that divalent cations, particularly copper, block M2 current [16] binding in the His37-Trp41 side chain quadruplex [17], divalent copper complexes of AMT were synthesized and found to be effective influenza A inhibitors with reduced cytotoxicity compared to CuCl_2 [15]. Because Cu^{2+} binds strongly to imidazole, it was suggested that the Cu^{2+} complexes also block M2 through His37-imidazole binding. In addition, the His37 cluster is highly conserved in nature [18], making it a prime target in the M2 channel.

The copper ligands developed were based on AMT and the lesser-known, equally effective M2 WT blocker, cyclooctylamine (CO) [19, 20], and extended via the amine with the functional groups iminodiacetate or iminodiacetamide. Six Cu^{2+} complexes (**Figure 1**) were synthesized and characterized using NMR, IR, MS, UV-Vis, and ICP-MS. The complexes demonstrated H37-specific block of M2 current in two electrode voltage-clamp (TEVC) studies with low μM potencies. The copper-free ligands did not show proton current block, demonstrating that the copper was key to the current-blocking process [15].

Because of the reduced toxicity to cultured cells found previously, we were interested to learn whether the six metal complexes were toxic to simple organisms. Zebrafish embryos were chosen because they have immune and nervous systems similar in many ways to more advanced organisms, because they are in an early, vulnerable stage of development, and because the compounds are readily administered at infection-relevant concentrations in their bathwater. We also explored and report additional properties of these copper complexes, including their efficacies in the cytopathic effect antiviral assay, their binding to albumin, mutagenicity testing in a bacterial assay, virus resistance development when passaged with cell culture in the presence of the compounds, and molecular dynamics simulations to explore how well the compounds fit in the M2 channel.

2. Materials and methods

2.1 Cytopathic effect assay

Confluent MDCK cells were transferred into 60 wells of a 96-well plate in DMEM (Gibco Thermo Scientific Waltham, MA, 4.5 g/L D-Glucose) with 5% Fetal Bovine Serum (FBS, Hyclone, Logan, UT). The cells were washed with a diluted solution of 50% SEM/50% serumless DMEM. SEM (simple electrolyte medium) consists of 4.33 g NaCl, 0.244 g KCl, 0.103 g $\text{CaCl}_2 \cdot 2\text{H}_2\text{O}$, $\text{MgCl}_2 \cdot 6\text{H}_2\text{O}$, $\text{Na}_2\text{HPO}_4 \cdot 7\text{H}_2\text{O}$, $\text{NaH}_2\text{PO}_4 \cdot \text{H}_2\text{O}$ in 500 ml H_2O . The cells were incubated for an hour with activated A/WS/33 virus and then the media with virus was removed. The SEM/serumless DMEM with 100 μM metal complex was added to six wells. The complexes were then serial-diluted in two-fold increments six times. Six wells were used as positive controls with no complex or virus added. Six wells were used as negative controls with only virus

added and no complex. About 80 μM ribavirin (Sigma-Aldrich, St. Louis, MO) was added to six wells as a positive control. The plates were incubated for 48 h at 33°C.

The crystal violet staining technique described previously [21] was used to determine the fraction of cells that survived the exposure to the virus. After 48 h, the test medium was removed, and the cells were washed three times with 150 μl PBS. The cells were stained for 10 min with 50 μl crystal violet solution (0.03% crystal violet (w/v) in 20% methanol). The cells were then washed three times with 150 μl distilled water before adding 100 μl lysis buffer. After 20 min, the optical density (OD) of each well was measured at 590 or 620 nm and averaged over the set of six wells for each concentration.

Because viral dosing was sufficient to eliminate essentially all cells in treatment-free controls, their average OD was subtracted as baseline from the average of the treated well ODs. The result was divided by the average of the uninfected control well ODs to obtain a normalized vitality. Because the vitality can be affected by both reduction of virus cytopathic effect and increase of treatment toxicity as concentration is increased, we fitted the normalized concentration-dependent vitality, $V(C)$, with a joint probability function:

$$V(C) = \frac{1}{1 + \left(\frac{EC_{50}}{C}\right)^{n_1}} \frac{1}{1 + \left(\frac{C}{CC_{50}}\right)^{n_2}} \quad (1)$$

Here, EC_{50} is the 50% effective dose of treatment that prevents viral cytopathic effect, CC_{50} is the 50% cytotoxic dose of the treatment, and n_1 and n_2 are their respective Hill coefficients. If the selectivity index, CC_{50}/EC_{50} , and the Hill coefficients are sufficiently high, this function rises to unity at doses that are sufficient to prevent viral replication but below toxic levels. Non-linear least squares fitting weighted with standard errors of means was done with the Marquardt algorithm in KaleidaGraph4 (Synergy Software, Reading, PA). In practice, it was necessary to fix the Hill coefficients to evaluate the effective doses, then manually adjust the Hill coefficients to improve the fit (due to low numbers of data points). Hence, the reported standard errors of the parameters obtained from the error matrix may be underestimated.

2.2 Protein binding assay

Each copper complex was dissolved in 25 ml of water to obtain a 1 mM and 800 μM solution. All water used in the protein binding assay was collected from a Millipore first-generation beige Milli-Q system. These solutions were sonicated until the crystals were fully dissolved. Four 1:2 serial dilutions were performed from the 800 μM solution to obtain 400, 200, 100, and 50 μM solutions, and a 1:5 dilution was performed from the 50 μM solution to obtain a 10 μM solution. 13.3 mg of BSA was then dissolved in 10 ml of each solution. The solutions were mixed thoroughly and allowed to stand at room temperature for approximately 20 min.

Spin filtration was performed using a swinging bucket rotor at 4000 rpm for 6 min. The spin filters used were Amicon Ultra-15 centrifugal filters. The filtrates from each spin were collected to test for copper content in ICP-MS. Solutions for ICP-MS were prepared from both the original solutions and the filtrates. For each solution, 1 ml of solution was added to 1 ml of 4% HNO_3 and 8 ml of 2% HNO_3 to obtain a 1:10 dilution of each solution in 2% HNO_3 . Nitric acid used for ICP-MS analysis was OmniTrace trace-metal grade obtained from EMD Millipore Corporation. We used BSA to model copper binding histidine in solution and calculate relative dissociation constants (K_d) for each complex. Copper

concentrations were obtained using ICP-MS. The data was fit to Eq. (2) to estimate K_d and the number of binding sites, n .

$$\frac{[Cu]_i - [Cu]_f}{[P]_i} = \frac{n * [Cu]_f}{K_d + [Cu]_f} \quad (2)$$

2.3 Zebrafish toxicity test

Following an approved BYU IACUC protocol, two AB wild-type male and female zebrafish were placed in an embryo media filled tank. The fish remained in a light and temperature-controlled facility until the following morning. Later that day, the fish were transferred into original tank. Embryos were moved into embryo media filled petri dishes (60 embryos/dish) and housed in an incubator for 2 days. Media was changed daily.

Fish embryos were dechorionated at 48 hpf. In a multi-well plate, 10 embryos were selected and 5 were added to each of two wells for each concentration with fresh embryo media. Drug solution (0–200 μ M) was then added to test toxicity and observed over 5 days. Drug solutions were changed daily. After 5 days, the fish were scored using a morbidity scale (**Table 1**) indicating response, spine shape, edema, equilibrium, and death. The average for each complex was normalized using the maximal morbidity score of 50/well. The fish were then euthanized.

2.4 Ames testing

The Modified Ames ISO kit (Environmental Bio-Detection Products Inc., Mississauga, ON) was used with *S. typhimurium* TA100 (no S9 fraction).

The complexes were compared against the mutagenicity of a positive control (NaN_3) and vehicle (water). The complexes were serially diluted 1:2 to compare the complexes' mutagenic ability at each of six concentrations.

TA100 was hydrated and incubated with histidine overnight at 37°C. Following the kit's instructions, in 96-well plates' exposure solution, diluted bacteria mix, and serial two-fold dilutions of complexes were combined with reversion media containing Bromocresol Purple, which serves as a pH indicator to identify infected wells. The 96 well plates were incubated for 6 days at 37°C without agitation. When a sample is mutagenic, it will revert the bacteria to WT, causing the media to turn slightly acidic and show a yellow color.

The number of reverted wells with complex was compared to the average number of reverted wells in the negative control. Significance was calculated using a one-tailed t-test.

2.5 Simulations

The 2KQT M2 structure was used and oriented in a DMPC lipid bilayer with a center-of-mass harmonic constraint. The copper complexes were oriented such that the copper was near (~ 2.0 Å) at least one of the four imidazole nitrogens. Water molecules within 2.2 Å of the complexes were deleted. The protein-bilayer system was solvated with a tetragonal 60 Å \times 60 Å \times 90 Å water box as shown in **Figure 2**. The system was minimized for 1000 steps of steepest descent and heated to 300 K. The M2 channel was equilibrated for 1 ns. The complexes were pulled using a constant force for 10 ps during the production runs. Frames were saved every 50 steps, which is every 50 fs, of production for a total of 200 frames. Standard CHARMM version 37b1 parameters were used. Copper dihedral parameters were created using a 20 kcal/mol/rad² energy penalty, which kept a conservatively rigid structure throughout the channel (**Table A1**).

Zebrafish scoring indicators				
Morbidity points	0	1	2	3
Equilibrium	Upright position	Lying on side	NA	NA
Response	Quick escape	Sluggish escape	No escape	NA
Spine shape	Straight	Slightly curved	Strongly curved	NA
Edema	None	1 place and minor	2 places or major	2 places and major
Death	=10			
Five fish per group in each of two wells.				

Table 1.
Scoring indicators observed daily for 5 days.

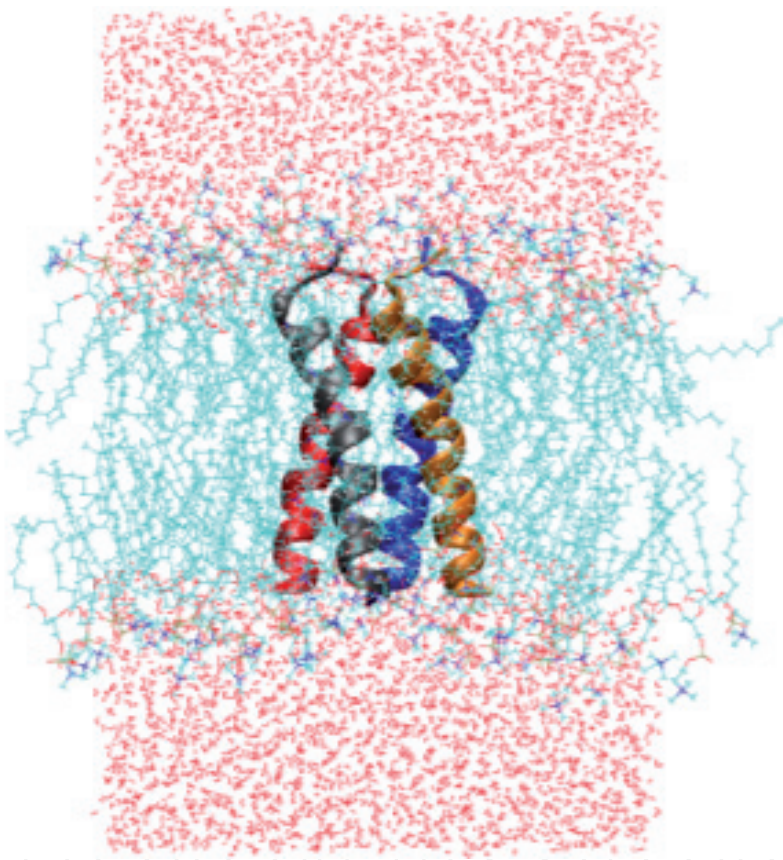


Figure 2.
Solvated DMPC-2KQT system.

The distance between imidazole nitrogens and copper on the complexes was calculated using CHARMM’s CORREL subroutine for each frame. The time for each complex was recorded when the copper reached 30 Å away from the imidazole nitrogens. This distance was chosen to represent the complex leaving the mouth of the channel.

2.5.1 Decisions affecting pulling force

The pulling force for each of the complexes was determined by normalizing the pulling forces to a 2.34 nN pulling force on AMT. The 2.34 nN force allowed comparisons to be made between compounds as they left the channel on the 10 ps timescale.

These steered molecular dynamics (SMD) simulations were analyzed by computing the mean and standard deviation of five independent. The five independent simulations were assigned random starting velocities and then analyzed to explore the time needed to pass the 30 Å threshold relative to the starting point from the copper atom on the complex.

The analysis examined whether the pulling forces, copper ligation mechanism, or scaffold (CO, AMT, or neither), significantly affected the exit times relative to free Cu^{2+} .

2.6 Miniplate assays, resistance testing, and sequencing

MDCK cells were seeded into a six-well plate and grown in Dulbecco's Modified Eagles Medium (DMEM, Sigma-Aldrich, St. Louis, MO) augmented by 5% with fetal bovine serum (FBS, Hyclone, Logan, UT) until confluent. After 48 h, the growth media was removed and replaced with DMEM. At this point the virus (A/CA/07/09) was introduced into the medium (200 pfu/ml) and allowed to adsorb for 1 h. The medium was then removed and replaced with fresh DMEM containing a specified concentration of complex and 5 ml of tosyl phenylalanyl chloromethyl ketone (TPCK)-treated trypsin (Thermo-Fischer Scientific, Waltham, MA, 1 mg/ml) was added to activate the virus. The plate was incubated at 33°C for 3 days. Then the medium was removed and centrifuged at 2000 rpm in order to remove cell debris. This virus-containing medium was then separated into 1-ml aliquots and frozen in Eppendorf tubes at -80°C. This process was repeated for each successive passage.

The concentration of virus was determined through an immunofluorescence assay (as previously described by [22]), which gave a multiplicity of infection (MOI) of 0.6. MDCK cells were seeded onto glass coverslips in vials containing 1 ml DMEM and trypsin in order to obtain 90% confluency after 24 h. The cells were allowed to grow overnight at 37°C, after which the growth medium was removed and replaced with DMEM. The sample of virus was then diluted by factors of 10, and the various dilutions of virus were stirred into the vials with coverslips. They grew at 33°C for 18 h. After this incubation period, the medium was removed, the cells were fixed with cold acetone (-80°C), and the coverslips were washed and stained with a fluorescein isothiocyanate labeled anti-IAV monoclonal antibody (Millipore Sigma, Burlington, MA, Cat. #5017). Excess antibody was washed off using a solution of 0.05% Tween20 in phosphate buffered saline and then again with distilled water. They were then viewed microscopically and individual infected cells (miniplates) were counted.

This same process was followed in determining the new EC_{50} against the specific complex of each resistant strain. Except, 100 pfu of virus was used in each vial. Several different concentrations of the complex with which it was passaged were introduced into the vials, with concentrations ranging from 2 to 70 μM . The cells were infected with the virus in a solution of SEM rather than DMEM. The EC_{50} was calculated in KaleidaGraph using the Levenberg-Marquardt algorithm. The fitting parameters (sigmoidal function) were used to calculate the EC_{50} and the standard error of the mean.

To sequence the genome, the viral sample was concentrated 10-fold using a spin filter (VWR North America, Radnor, PA, Cat. #82031-352). After that, viral RNA was isolated using the QIAamp Viral RNA Mini Kit (Qiagen, Germantown, MD). The isolated RNA was stored at -20°C. RNA was then reverse-transcribed using Invitrogen's Superscript III One-Step RT-PCR Platinum Taq HiFi kit (Thermo-Fischer Scientific, Waltham, MA).

The resulting isolated DNA was stored at -20°C. The DNA was then amplified with PCR using the Phusion High-Fidelity PCR kit (New England Biolabs, Ipswich, MA). The solution was purified using Qiagen's QIAquick PCR

Purification Kit (Qiagen, Germantown, MD). It was sequenced using custom forward (TGTAACGACGGCCAGTACGAAAAGCAGGTAG) and reverse (CAGGAAACAGCTATGACCAGTAGAAACAAGGTAGT) primers for the segment of the new DNA that codes for the M2 protein.

3. Results and discussion

3.1 Cytopathic effect assay

Although 1–4 had good potency against initial infections in the immunofluorescence (miniplaque) assay [15], the copper complexes had no effect in the cytopathic effect (CPE) assay with MDCK cells when dissolved in serumless DMEM. However, when the serumless DMEM was diluted with SEM, 1 (**Figure 3**) and to a lesser extent 3 (data not shown) exhibited cell protection. Using a dual-sigmoidal function curve fit, 1 has an EC_{50} of $0.9 \pm 0.08 \mu\text{M}$ and a CC_{50} of $5.8 \pm 0.37 \mu\text{M}$. The submaximal efficacy is due to high cytotoxicity. The selectivity index for 1 is 6.44, given by the ratio of the CC_{50} and EC_{50} . The low EC_{50} compares favorably to the EC_{50} in the miniplaque assay, $6.7 \pm 1.2 \mu\text{M}$. In contrast, 3 has an EC_{50} greater than $100 \mu\text{M}$, whereas its potency in the miniplaque assay was $EC_{50} = 0.7 \pm 0.1 \mu\text{M}$, and 2 and 4–6 showed no effect, indicating that other factors were involved. The fact that some efficacy is observed when the medium is diluted with amino-acid free SEM suggests that free amino acids in non-dilute DMEM interfere with the copper complex efficacy.

3.2 Protein binding assay

To illustrate the potential of the metal complexes to bind to proteins, binding to BSA was measured in which a protein solution was mixed with various concentrations of a CuCl_2 or copper complex solution. The copper content of the original sample

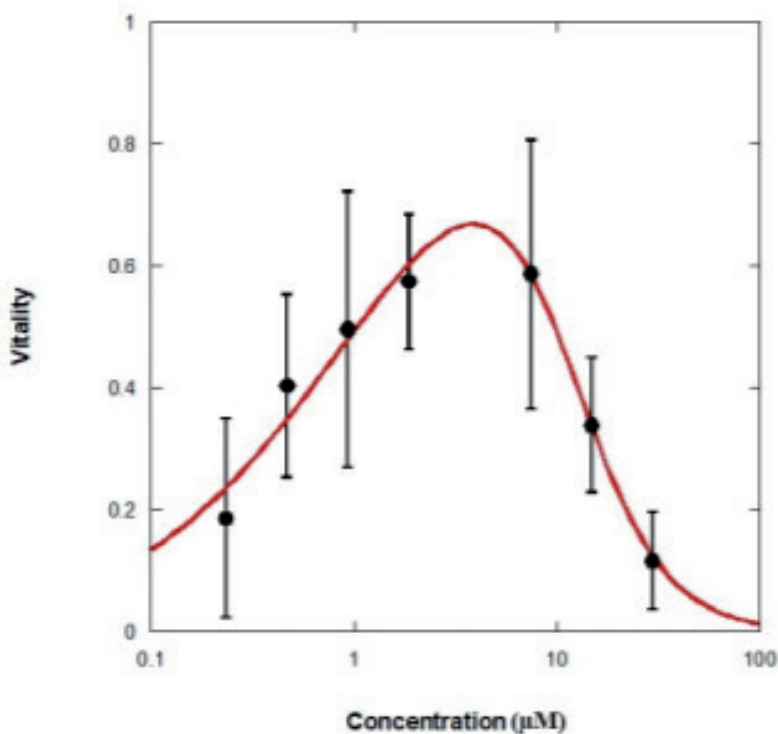


Figure 3.
CPE assay showing protective effect of 1 against A/WS/33 (M2 S31N) infection of MDCK cells using dilute medium (50% DMEM, 50% SEM). MOI 0.6; 48-h incubation.

was measured and compared to that of the filtrate. Taking the volume proportions into account, the “free copper concentration” in the filtrate relative to the “total copper concentration” in the original sample was fitted to a model assuming that each protein molecule had n equivalent copper or copper complex binding sites. **Table 2** shows the best fit K_d values, assuming that each albumin monomer has n equivalent binding sites. The two parameters interacted and were therefore poorly constrained in the optimization of the deviations squared, but **Table 2** indicates that the number of binding sites is well above 10, consistent with the count of 13 surface histidines in monomeric albumin (**Figure A1**). Complexes **1**, **3**, and **5** have larger K_d values compared to that of CuCl_2 (59.1 μM). This indicates that the ligands on the metal complexes reduce the binding affinity for albumin binding sites, but also still allow for substantial binding. It is also consistent with the electrophysiology results for blocking through binding of copper complex to the His37 cluster in the M2 channel.

BSA has 13 surface histidines (**Figure A1**), however, all of the fits optimized n at >13 copper binding sites. This difference could suggest non-specific binding to other sites on BSA. The high K_d 's for the complexes relative to CuCl_2 indicate that the complexes remain intact during binding to BSA. The binding the copper complexes to BSA is very weak compared to that of the $\text{M}_2\text{S}_{31}\text{N}$ (AMT resistant) channel, where block was $\sim 80\%$ for **1** and **3** after 57 and 27 min perfusion, respectively. This suggests that protein binding *in vivo* would be a minor concern. However, it is clear that binding by non-M2 proteins is detectable and, given their large quantity inside and outside the blood, they could limit access of the copper complexes to virus.

3.3 Zebrafish toxicity test

Toxicity was evaluated for zebrafish exposed to various concentrations of CuCl_2 or copper complex (**1–5**) added as methanolic solutions to the embryo bath medium starting 48 h post fertilization (Day 0) (**Figure 4**). At 200 μM copper complex on day 1, compounds **2**, **4**, and **5** show minimum toxicity effects, **1** and **3** show moderate toxicity including slow response to stimulation, slightly curved spine, and minor edema, whereas CuCl_2 causes major edema, strongly curved spine, no response to stimulation, and death. By day 2 at 200 μM , the toxicities of **1**, **2**, **4**, and **5** have increased moderately but still only moderate spine curvature and minor edema, while **3** causes slow response to stimulation, strongly curved spine, and moderate to major edema. By days 3, 4, and 5 at 200 μM , all but **5** show low or no response, strongly curved spines, major edema, and some death. The MeOH vehicle controls showed statistically insignificant toxicity.

Compared to CuCl_2 , the copper complexes show less toxicity, suggesting that the ligands are coordinating to the copper and helping to reduce its toxicity through day 2 of high dosage. All of the copper complexes produce some toxicity in the zebra fish for all experimental concentrations, but compound **5** does not increase in

Complex	K_d (μM)	Sites (n)
CuCl_2	59.1	15
1	128.7	19
3	179.5	20
5	380	20*

*K_d values for representative compounds **1**, **3**, and **5**. *The value of n was not well-constrained and was therefore fixed during the curve fit.*

Table 2.
Binding to bovine serum albumin results.

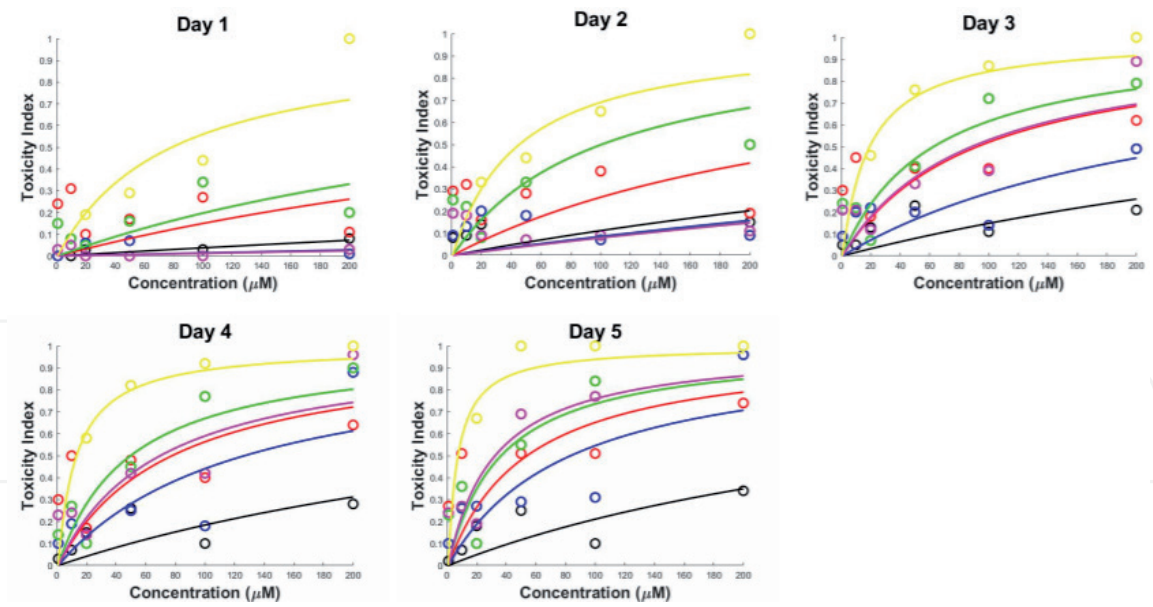


Figure 4. Zebrafish toxicity of copper complexes. CuCl₂ (yellow), 1 (red), 2 (blue), 3 (green), 4 (magenta), 5 (black). (Arbitrary toxicity index, see Section 2).

toxicity over time as much as the other complexes. This suggests further testing and modification of compound 5 could lead to a safe anti-influenza A therapeutic.

3.4 Ames testing

The mutagenicity of the copper complexes was tested using the Ames test. **Table 3** shows the percent reversion out of 48 wells of three complexes. They were tested for mutagenicity against *S. Typhimurium* TA100, which strain of bacteria allows a test for mutagenicity caused by base-pair substitution and oxidative damage. The percent of revertant wells (reversion rate) was compared against the negative control and found to be statistically insignificant ($p > 0.01$). The positive control (NaN₃) had an average 91.7% reversion rate compared to the negative control’s average rate of 43.8% ($p < 0.0001$). Complexes 1, 3, and 4 did not show significant rate of reversion at any tested concentration compared to NaN₃. The copper complexes showed approximately the same reversion rates as the negative control after 6 days. Therefore, they do not cause mutagenicity due to base-pair substitution or oxidative damage.

Concentration (μM)	Complex		
	1	3	4
500	42	42	50
250	42	42	30
125	31	52	33
62.5	31	41	38
31.25	52	58	67
15.63	56	52	56
0	35	46	50

Percent of reversion out of 48 wells for compounds 1, 3, and 4 for concentrations between 15 and 500 μM. 0 is water with no complex.

Table 3. Ames mutagenicity assay results.

3.5 Resistance testing and sequence

Because the putative target for the metal complexes, the His37 quadruplex, is highly conserved in nature and functionally critical for vRNP uncoating, we explored the propensity for virus resistance formation with passaging in MDCK cell cultures. Because the incubation had to be done in DMEM, which is known to inhibit complex efficacy, we used higher concentrations of complexes for the incubations such that the efficacy of block was projected to be ~50%, thus creating a concentration where mutation could occur. Ten passages (~5 weeks) of incubated virus in DMEM dosed with increasing metal complex concentrations (ranging from 50 to 100 μM) was chosen as a rigorous test. Resistance would be identifiable by an increase in miniplaque EC_{50} after passaging relative to the original value. As shown in **Table 4**, the new EC_{50} (column 3) is comparable to the original EC_{50} (column 2). Because none of the copper complexes significantly increased the EC_{50} after 5 weeks of incubation, we conclude that resistance is slow to develop. This contrasts with rapid resistance development when passaging with AMT [15].

The vRNA M segment was extracted from the passaged virus exposed to **3**, sequenced and compared to A/CA/07/2009 using a reverse-BLAST mechanism. The only base mutation discovered was G749A, which translates to the amino acid mutation G16E. This amino acid is positioned in the region of the channel entry that is outside of the membrane and unlikely to influence channel permeation. According to the results in the above table, this mutation did not confer resistance to this compound. We consider the occasionally observed natural M2 mutant G34E to be likely to escape block by these complexes. Although we did not see resistance develop in our assays, a more direct assessment of the G34E site mutation using electrophysiology might be instructive about resistance potential for these compounds in future studies.

3.6 MD simulations

Constant force steered molecular dynamics (MD) simulations were carried out to explore the steric limitations on metal complex exit from the M2 transmembrane domain AMT binding site. A 2.34 nN force was used to pull the complexes pass the 30 Å threshold and beyond the Val27 cluster within 10 ps. The 2.34 nN force gave a sufficient spread in leaving times to allow assessment of the ease of unbinding relative to AMT. For these simulations, the force was applied to the center-of-mass of the complex. Example trajectories for AMT (green) and **4** (yellow) are shown in **Figure 5**. The starting configurations (left) had the adamantyl groups of AMT and **4** superimposed with the copper atom of **4** oriented down, close to H37. This binding configuration was used for all of the metal complexes. V27 and H37 are shown as reference points along the channel.

Complex	Original A/CA/09 (μM)	10 passages with complex (μM)
1	6.9 ± 1.2	3.7 ± 0.5
2	4.9 ± 0.8	2.1 ± 1.1
3	0.7 ± 0.1	1.1 ± 0.4
4	11.6 ± 1.1	3.9 ± 6.8
5	8.2 ± 2.0	1.3 ± 0.2
6	4.4 ± 0.6	2.9 ± 0.3

DMEM was used for passage incubations and SEM for the miniplaque assays.

Table 4.
Miniplaque $\text{EC}_{50} \pm \text{SE}$ (EC_{50}) before (original) and after 10 passages of virus in MDCK cells.

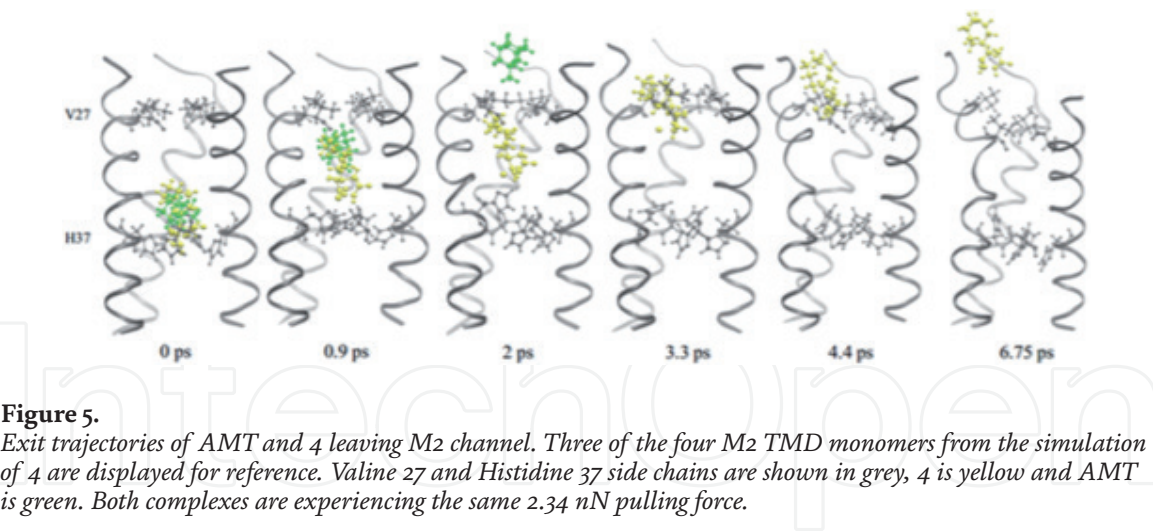


Figure 5. Exit trajectories of AMT and 4 leaving M2 channel. Three of the four M2 TMD monomers from the simulation of 4 are displayed for reference. Valine 27 and Histidine 37 side chains are shown in grey, 4 is yellow and AMT is green. Both complexes are experiencing the same 2.34 nN pulling force.

Complex	Average time to leave (ps)
1	4.60 ± 1.14
2	6.85 ± 1.01
3	4.67 ± 1.07
4	7.05 ± 0.53
5	3.75 ± 0.89
6	4.00 ± 1.06
AMT	2.77 ± 0.26

Table 5. Average time to leave (±standard deviation) the channel with a 2.34 nN force applied to the compound's center-of-mass.

Table 5 shows the average time to leave from five independent simulations (identical starting configurations, but randomly assigned atomic velocities) for each complex to pass the 30 Å threshold. All metal complexes took longer to leave the channel than AMT. AMT exited the channel in 2.77 ps. Complex 4 interacts with the V27 side chain and was the slowest compound to leave the channel, with its leaving time at 7.05 ps. By 4.4 and 6.75 ps, some distortion is seen on the protein subunit as 4 is pulled further out of the channel.

4. Conclusion

The copper complexes are relatively non-toxic in zebrafish embryos compared to CuCl₂ over a 5-day period. Also, they are efficacious in a 3-day assay (but with limitations due to serum protein binding and amino acid interference), are non-mutagenic compared to sodium azide, are slower to leave the M2 binding site compared to AMT, and, also compared to AMT, are not prone to resistance development. *In vivo* they would face competition with binding to other proteins and the therapeutic window is small. However, complexation of copper could be pharmacologically beneficial.

Further testing of these copper complexes should include isothermal titration calorimetry (ITC) experiments with influenza A M2 channel to obtain binding energies, two-electrode voltage clamp (TEVC) experiments to obtain rate constants of binding to M2, and testing in an animal model that more accurately represents the effects of the copper complexes on humans.

Appendix

See **Figure A1** and **Table A1**.

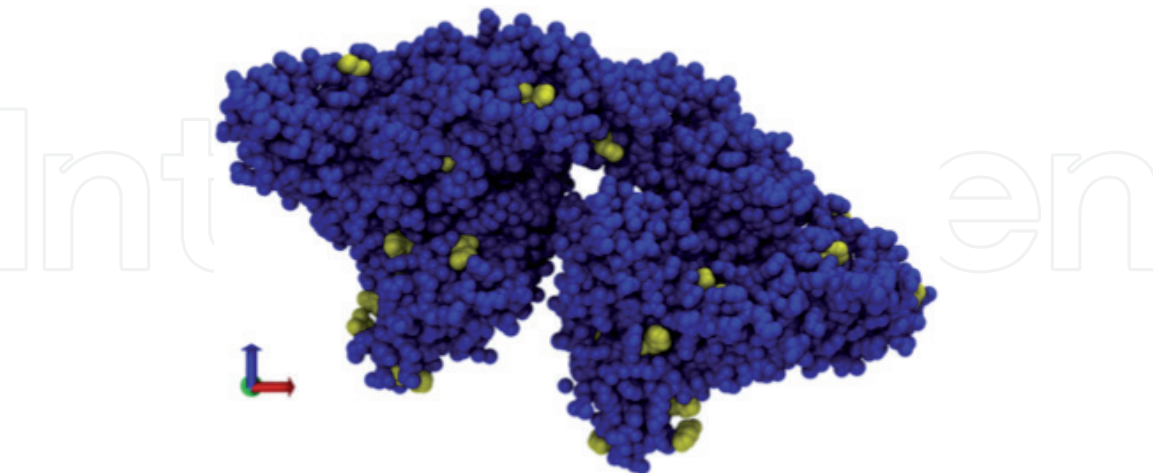


Figure A1.
Bovine serum albumin view (RCSB 3Vo3). Histidine side chains are colored yellow.

CU parameters			
Bond	Kb (kcal/mol/Å2)	B0 (Å)	
CU-N	270.2	2.026	
Angle	Kθ (kcal/mole/rad2)	θ0 (degrees)	
CT1-NPH-CU	96.150	128.05	
HB1-NPH-CU	30	123	
CT2-NH3-CU	96.150	128.05	
H-NPH-CU	0	180	
NPH-CU-NH3	14.39	90	
NPH-CU-NPH	14.39	90	
Dihedral	Φ (kcal/mole/rad2)	Multiplicity	Delta (degrees)
NPH-CU-NH3-CT2	20	1	92.30
CU-NPH-C2-OB	20	2	169.1
CU-NH3-CT1-CT2	20	1	-58.6
H-NPH-CU-NH3	20	2	157.9
NPH-CU-NPH-H	20	2	161.2
H-NPH-CU-NH3	20	2	157.9
C2-NPH-CU-NPH	20	2	18.8
CU-NPH-C2-CT2	20	2	8.0
CU-NH3-CT2-HA	20	3	90.20
C2-CT2-NH3-CU	20	2	-30.80
NPH-CU-NH3-H	20	2	161.2

Table A1.
CHARMM copper parameters.

IntechOpen

Author details


Kelly L. McGuire¹, Jon Hogge¹, Aidan Hintze¹, Nathan Liddle¹, Nicole Nelson¹, Jordan Pollock¹, Austin Brown¹, Stephen Facer¹, Steven Walker¹, Johnny Lynch², Roger G. Harrison^{2*} and David D. Busath^{1*}

¹ Department of Physiology and Developmental Biology, Brigham Young University, Provo, UT, USA

² Department of Chemistry and Biochemistry, Brigham Young University, Provo, UT, USA

*Address all correspondence to: roger_harrison@byu.edu and david_busath@byu.edu

IntechOpen

© 2019 The Author(s). Licensee IntechOpen. This chapter is distributed under the terms of the Creative Commons Attribution License (<http://creativecommons.org/licenses/by/3.0>), which permits unrestricted use, distribution, and reproduction in any medium, provided the original work is properly cited. 

References

- [1] Busath DD. Influenza A M2: Channel or Transporter? *Advances in Planar Lipid Bilayers and Liposomes*. Vol. 10. Burlington: Academic Press; 2009. pp. 161-201
- [2] Chizhmakov IV, Geraghty FM, Ogden DC, Hayhurst A, Antoniou M, Hay AJ. Selective proton permeability and pH regulation of the influenza virus M2 channel expressed in mouse erythroleukaemia cells. *The Journal of Physiology*. 1996;**494**(Pt 2):329-336
- [3] Helenius A. Unpacking the incoming influenza virus. *Cell*. 1992;**69**(4):577-578
- [4] Venkataraman P, Lamb RA, Pinto LH. Chemical rescue of histidine selectivity filter mutants of the M2 ion channel of influenza A virus. *The Journal of Biological Chemistry*. 2005;**280**(22):21463-21472
- [5] Wang C, Lamb RA, Pinto LH. Activation of the M2 ion channel of influenza virus: A role for the transmembrane domain histidine residue. *Biophysical Journal*. 1995;**69**(4):1363-1371
- [6] Davies WL, Grunert RR, Haff RF, McGahen JW, Neumayer EM, Paulshock M, et al. Antiviral activity of 1-adamantanamine (amantadine). *Science*. 1964;**144**(3620):862-863
- [7] Krylov VF, Alekseeva AA, Liarskaia T, Poliakova TG, Kupriashina LM. Therapeutic effectiveness of bonafton and rimantadine in influenza. *Voprosy Virusologii*. 1976;(2):186-191
- [8] Wang C, Takeuchi K, Pinto LH, Lamb RA. Ion channel activity of influenza A virus M2 protein: Characterization of the amantadine block. *Journal of Virology*. 1993;**67**(9):5585-5594
- [9] Hata M, Tsuzuki M, Goto Y, Kumagai N, Harada M, Hashimoto M, et al. High frequency of amantadine-resistant influenza A (H₃N₂) viruses in the 2005-2006 season and rapid detection of amantadine-resistant influenza A (H₃N₂) viruses by MAMA-PCR. *Japanese Journal of Infectious Diseases*. 2007;**60**(4):202-204
- [10] Krumbholz A, Schmidtke M, Bergmann S, Motzke S, Bauer K, Stech J, et al. High prevalence of amantadine resistance among circulating European porcine influenza A viruses. *The Journal of General Virology*. 2009;**90**(Pt 4): 900-908
- [11] Balannik V, Wang J, Ohigashi Y, Jing X, Magavern E, Lamb RA, et al. Design and pharmacological characterization of inhibitors of amantadine-resistant mutants of the M2 ion channel of influenza A virus. *Biochemistry*. 2009;**48**(50):11872-11882
- [12] Wang J, Ma C, Wang J, Jo H, Canturk B, Fiorin G, et al. Discovery of novel dual inhibitors of the wild-type and the most prevalent drug-resistant mutant, S₃₁N, of the M2 proton channel from influenza A virus. *Journal of Medicinal Chemistry*. 2013;**56**(7):2804-2812
- [13] Wu Y, Canturk B, Jo H, Ma C, Gianti E, Klein ML, et al. Flipping in the pore: Discovery of dual inhibitors that bind in different orientations to the wild-type versus the amantadine-resistant S31N mutant of the influenza A virus M2 proton channel. *Journal of the American Chemical Society*. 2014;**136**(52):17987-17995
- [14] Zhao X, Jie Y, Rosenberg MR, Wan J, Zeng S, Cui W, et al. Design and synthesis of pinanamine derivatives as anti-influenza A M2 ion channel inhibitors. *Antiviral Research*. 2012;**96**(2):91-99
- [15] Gordon NA, McGuire KL, Wallentine SK, Mohl GA, Lynch JD,

Harrison RG, et al. Divalent copper complexes as influenza A M2 inhibitors. *Antiviral Research*. 2017;**147**:100-106

[16] Gandhi CS, Shuck K, Lear JD, Dieckmann GR, DeGrado WF, Lamb RA, et al. Cu(II) inhibition of the proton translocation machinery of the influenza A virus M2 protein. *The Journal of Biological Chemistry*. 1999;**274**(9):5474-5482

[17] Su Y, Hu F, Hong M. Paramagnetic Cu(II) for probing membrane protein structure and function: Inhibition mechanism of the influenza M2 proton channel. *Journal of the American Chemical Society*. 2012;**134**(20):8693-8702

[18] Durrant MG, Eggett DL, Busath DD. Investigation of a recent rise of dual amantadine-resistance mutations in the influenza A M2 sequence. *BMC Genetics*. 2015;**16**(Suppl. 2):S3

[19] Pinto CA, Haff RF. Antiviral activity of cyclooctylamine hydrochloride in influenza virus-infected ferrets. *Antimicrobial Agents and Chemotherapy*. 1968;**8**:201-206

[20] Lin TI, Heider H, Schroeder C. Different modes of inhibition by adamantane amine derivatives and natural polyamines of the functionally reconstituted influenza virus M2 proton channel protein. *The Journal of General Virology*. 1997;**78**(Pt 4):767-774

[21] Schmidtke M, Schnittler U, Jahn B, Dahse HM, Stelzner A. A rapid assay for evaluation of antiviral activity against coxsackievirus B3, influenza virus A, and herpes simplex virus type 1. *Journal of Virological Methods*. 2001;**95**:133-143

[22] Kolocouris A, et al. Amino-adamantanes with Persistent in Vitro Efficacy against H1N1 (2009) Influenza A. *Journal of Medicinal Chemistry*. 2014;**57**(11):4629-4639